

An effective approach for analysis of shoreline change and determination of its future location using satellite imagery: A case study of the Lake Burdur, Turkey

Uydu görüntüleri kullanılarak kıyı şeridi değişimi analizi ve gelecekteki konumunun belirlenmesi için etkili bir yaklaşım: Burdur Gölü örneği

Amine KOÇ¹ , Nuray BAŞ^{*1} 

¹Sivas Cumhuriyet University, Department of Geomatics Engineering, 58140, Sivas, Turkey

• Received: 03.03.2023

• Accepted: 23.10.2023

Abstract

Lake shoreline changes can have a significant impact on the biodiversity and ecosystems of wetland. This study was aimed to calculate the coastal change of Lake Burdur in Turkey during the elapsed period from 2013 to 2023. Within this framework both remote sensing based approach and Digital Shoreline Analysis System (DSAS) was performed using Landsat-7 (TM) and Landsat-8 (OLI) images. To estimate shoreline change rates along the coastal zone, statistical parameters such as End Point Rate (EPR), Linear Regression Rate (LRR), and Net Shoreline Movement (NSM) were calculated. A hybrid algorithm, Normalized Difference Vegetation Index (NDVI) and Tasseled Cap Analysis, is utilized to emphasize the distinction between the lake bodies and coastal zone. The maximum shoreline change in the northeast part of the lake was observed, and it resulted in a change of 543.12 m/yr for EPR and 610.07 m/yr for LRR statistics in the 2013-2023 time period. The lake to land position has only been observed in a small amount which are resulted in for EPR -4.91 m/yr. and -3.17 m/yr for LRR statistics. The lake area decreased from 139 km² to 118 km² between 2013 and 2023. The results indicate that if the decision-maker does not measure, the area of the lake will be lost by 14% until 2033 and 27% until 2043.

Keywords: Lake Burdur, Nsm-Epr-Lrr statistics, Shoreline change, Tasseled cap

Öz

Göl kıyı şeridi değişikliklerinin sulak alanın biyolojik çeşitliliği ve ekosistemleri üzerinde önemli etkileri bulunmaktadır. Bu çalışma, Türkiye'deki Burdur Gölü'nün 2013-2023 yılları arasındaki kıyı değişiminin belirlenmesi amaçlamıştır. Bu çerçevede Landsat-7 (TM) ve Landsat 8 (OLI) görüntüleri ile hem uzaktan algılama tabanlı yaklaşım hem de Sayısal Kıyı Şeridi Analiz Sistemi (DSAS) yöntemi kullanılmıştır. Kıyı bölgesi boyunca kıyı şeridi değişim oranlarını tahmin etmek için Son Nokta Oranı (EPR), Doğrusal Regresyon Hızı (LRR) ve Net Kıyı Şeridi Mesafesi (NSM) gibi istatistiksel parametreler hesaplanmıştır. Göl ile kıyı bölgesi arasındaki ayrımı vurgulamak için ise, Normalleştirilmiş Fark Bitki Örtüsü İndeksi (NDVI) ve Tasseled Cap Analizi adlı hibrit bir algoritma kullanılmıştır. En fazla kıyı şeridi değişikliği gölün kuzeydoğu kesiminde gözlenmiş olup, 2013-2023 dönemi için EPR değeri 543,12 m/yıl, LRR değeri ise 610,07 m/yıl olarak sonuçlanmıştır. Göl-kara yönünde meydana gelen değişim EPR -4,91 m/yıl ve LRR -3,17 m/yıl olarak yalnızca küçük bir miktarda gözlemlenmiştir. Göl alanı ise, 2013-2023 yılları arasında 139 km²'den 118 km²'ye kadar düşmüştür. Elde edilen sonuçlar, eğer otoritelerce önlem alınmazsa göl alanının 2033 yılına kadar %14, 2043 yılına kadar ise %27 oranında kayıp yaşayacağını göstermektedir.

Anahtar kelimeler: Burdur Gölü, Nsm-Epr-Lrr istatistikleri, Kıyı değişimi, Tasseled cap

*Nuray BAŞ; nuraybas@gmail.com

1. Introduction

The shoreline changes of wetlands play a critical role in ecosystems. Over time, the coastline undergoes significant changes due to exposure to nature (Wang et al., 2022) and anthropogenic factors (Addo, 2012). The effects of climate change on the world can be clearly observed due to global warming, which is defined as one of the biggest disasters. There are a lot of lakes/wetlands around the world that are in danger or have a significant decrease in water volume. One of them is Lake Burdur, which is under the influence of climate change and anthropogenic effects and is the seventh largest lake in Turkey.

In recent years, the dams built on the rivers and the use of water in agricultural activity, intense evaporation due to climate change have led to water loss and increased salinity in the Lake. Burdur Lake is an important ecosystem that hosts a large number of animals. Furthermore, it has great important wetland for birds wintering periods. For example, *Aphanius sureyanus* fish lives only in Lake Burdur (Tamer et al., 2020).

Lake Burdur has been consistently observed for years to examine the current situation and potential changes by the General Directorate of State Hydraulic Works. The first measurements were performed in 1959 and the water level was measured at 851.32 m. Over time, water levels have been increasing and decreasing. The lake's surface reached its highest point at 857.62 m in 1970, followed by 841.82 m in 2015 and 837.68 m in 2022. The main causes of negative impacts on the Lake can be identified as unplanned construction, artificial coastal backfill, agricultural irrigation, dam construction, unconscious groundwater use, and global warming. For example, Kale et al. (2019) found that the dam constructed in the Yeşilirmak Delta in Turkey had a major impact on the coastline.

A variety of methods are used to monitor coastal changes in literature. For example, Kuleli & Bayazıt (2022) have developed a methodology for measuring shoreline sustainability with phased approach using criteria indicator sets. Today, photogrammetric techniques have been widely used with the development of space technology (Carvalho et al., 2020; Amroini et al., 2009). The most significant one is remote sensing technology, which has included a lot of images. Low resolution image like Spot-Pan, Aster, Landsat, etc. are often preferred because they are not time-consuming and cost-effective (Mitri et al., 2020; Qiao et al., 2018). For example, Dervişoğlu et al. (2022) examined changes in the water surface from 1985 to 2020 using Sentinel-2 and Landsat images. Synthetic Aperture Radar (SAR) images (Pradhan et al. 2018) and UAV technology can be shown as for potential coastal analysis (Lowe et al., 2019).

To calculate shoreline positions of the Lake have been commonly used End Point Rate (EPR), Linear Regression Rate (LRR) and Weighted Linear Regression (WLR) statistical analysis (Mishra et al., 2021; Dey et al., 2021).

In recent years, several pixel-based classification methods have been widely used as an active research topic in the field of remote sensing. Iterative Self-Organizing Data Analysis (ISODATA) was first introduced by Ball and Hall in 1965 and has been used by many researchers (Abedisi et al., 2021; Santa et al., 2023). Similar to classification methods, a number of methods have been utilized as a water spectral index for shoreline detection. The Normalized Difference Water Index (NDWI), and Tasseled Cap were successfully applied the coastal areas (Aishi & Hasan 2022).

Many more countries, including Turkey, have been facing a reduced availability of surface water resources due to global warming. Understanding the changes in these resources from the past to the present can help us avoid facing dangerous situations in the future.

Our objective in this study is to accurately determine the future and most recent positions of Lake Burdur to overcome this problem. In this context, shoreline extraction of the Lake Burdur was carried out by using Net Shoreline Movement (NSM), End Point Rate (EPR) and Linear Regression Rate (LRR) statistical methods via DSAS tools. The analysis involved the use of Landsat images with time intervals (2013-2015-2017-2021-2023). Specific details of the study include:

- (1) To achieve a more efficient result of land/lake discrimination, the Normalized Difference Vegetation Index (NDVI) and Tasseled Cap combination were utilized.

(2) The future shoreline positions were forecast for Burdur Lake in the 2033–2043-time intervals.

This study's purpose was to provide advice to the authorities and draw attention to the danger of coastal retreat in Lake Burdur.

2. Material and method

The materials and methods used in the study are presented in the following chapters.

2.1. Study area and data

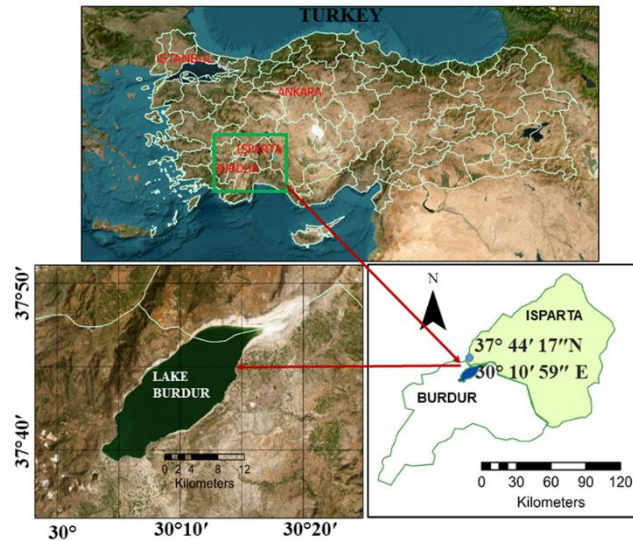


Figure 1. Location of the study area (a) geographic coordinates (b) Satellite image of Burdur Lake

Lake Burdur, located at the border between Burdur and Isparta provinces in Turkey, was chosen as the study area (Figure 1). This tectonic origin and large salinity lake is geographically located between 37° 44' 18" North Longitude and 30° 11' 00" East Latitude. Lake Burdur is one of the largest and deepest lakes in Turkey. The length of the distance is 34 km, and the width is 9 km. The elevation is 842.87 meters high. The water level was measured at 851.32 m for the first time in 1959. In 1970, this level reached its highest level at 857.62 m, but it has steadily decreased over time. The city settlements are situated to the east of Burdur Lake. The population is reported by TUIK as 273799 people (TUIK, 2022). Lake water is not used for domestic and agricultural purposes due to its high salinity and arsenic content. Despite the increase in precipitation since 1995, water levels are still declining due to the retention of stormwater in dams and ponds.

In this study, Landsat-7 (TM) and Landsat-8 OLI have been used as freely downloadable data from the United States Geological Survey (USGS) website (Table 1), (Survey, 2022). The resolution of the images is 15m panchromatic and 30m multispectral. These images were used by selecting the lowest cloud (10%) in terms of data quality. The data used in this study include the dates of 05/20/2013- 05/26/2015- 05/24/2017- 05/14/2019- 05/26/2021-04/30/2023. The month of May was chosen primarily because of the average rainy season.

Table 1. Satellite image properties used in study.

| Landsat-8 OLI/TIRS(2019-2021) Bands | Wavelength (μm) | Landsat 7 TM (2013-2017) Bands | Wavelength (μm) |
|---|---------------------------------|--------------------------------------|------------------------------|
| Panchromatic | | Panchromatic | 0.52-0.90 |
| Band 1-Coastal aerosol | 0.43-0.45 | Band 1-Blue | 0.45-0.52 |
| Band 2-Blue | 0.45-0.51 | Band 2-Green | 0.52-0.60 |
| Band 3-Green | 0.53-0.59 | Band 3-Red | 0.63-0.69 |
| Band 4-Red | 0.64-0.67 | Band 4-(Near-IR) | 0.77-0.90 |
| Band 5-(NIR) | 0.85-0.88 | Band 5-(Mid-IR) | 1.55-1.75 |
| Band 6-Swir-1 | 1.57-1.65 | Band 6-Termal-IR) | 10.31-12.36 |

2. 2. Method

Figure 2 presents the flow chart of the study's methodology.

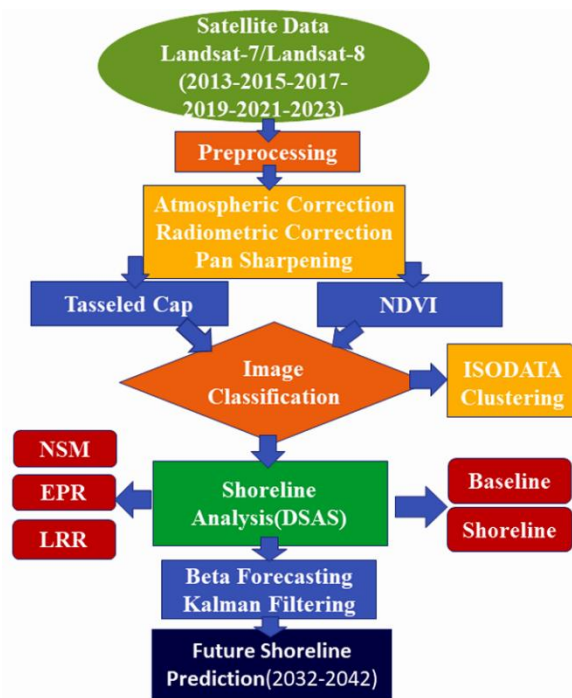


Figure 2. Flowchart of the proposed method

This study is divided into four stages. Preprocessing and image processing: Atmospheric and radiometric corrections and pan sharpening applications were applied to all Landsat images using QGIS software. To enhance the spatial resolution of the Landsat images, pan sharpening techniques were used. (2) Combined Tasseled Cap and NDVI analysis: In this study, the NDVI and Tasseled Cap combinations were used to determine the coastal boundary more clearly. The Tasseled Cap transformation and the process of wetness, brightness and greenness have been applied to all images. (3) Unsupervised Iterative Self-Organizing Data Analysis Technique (ISODATA) Classification: After the NDVI and Tasseled cap operations, ISODATA classification was applied to the composite images to generate classified images. (4) DSAS Analysis: The DSAS tool, an add-on to ArcGIS 10.4 software, was used to calculate the change rate of coastline line within the specified time interval. Finally, the Beta forecasting toolbox and the Kalman Filtering method were utilized to obtain coastal forecasting for the next 10 and 20 years.

2.2.1. Iterative Self-Organizing Data Analysis Technique (ISODATA), NDVI analysis and Tasseled Cap algorithm

Iterative Self-Organizing Data Analysis (ISODATA) is commonly utilized in remote sensing applications for large areas. This algorithm divides the image pixels into user-specific groups. Furthermore, the classified image was grouped into two categories (land and water). Before applying this process, atmospheric and radiometric corrections were performed on the image. To reduce errors, it is necessary to apply pre-processing steps to the image, including atmospheric and topographic effects, the angle of reflection from the sun, cloud effect, and shadow (Canbaz et al., 2018; Canbaz et al., 2017).

In the next steps the hybrid methods which were Tasseled cap and NDVI method was performed to enhance spectral discrimination of water body. Tasseled cap provides an analytical approach, giving measure of greenness, wetness and brightness of each pixel over a long or short time period. As a result, to increase the performance of the classifications, the spectral indices NDVI and brightness, greening and wetness Tasseled Cap process was carried out before the ISODATA classification (Samarawickrama et al. 2017). These processes were applied together in order to increase the sharpness between water and land on Landsat

OLI/TIRS satellite images belonging to the years 2013 - 2015 - 2017 -2019 - 2021 - 2023 (Eq.1,2,3,4) (Thieler et al. 2009). The Red (Band 4) ve NIR (Band 5) was applied in Equation1.

$$\text{NDVI} = (\text{Bant 5} - \text{Bant 4}) / (\text{Bant 5} + \text{Bant 4}) \quad (1)$$

$$\text{Brightness: } b1*0.3029+b2*0.2786+b3*0.4733+b4*0.5599+b5*0.508+b6*0.1872 \quad (2)$$

$$\text{Greenness: } b1*(-0.2941) +b2*(-0.243) +b3*(-0.5424) +b4*0.7276+b5*0.0713+b6*(-0.1608) \quad (3)$$

$$\text{Wetness: } b1*0.1511+b2*0.1973+b3*0.3283+b4*0.3407+b5*(-0.7117) +b6*(-0.4559) \quad (4)$$

In the second step, the shorelines were automatically extracted by assigning the value-1 as Id-1 to the bare earth class and as the value-2 as Id-2 to the water class using unsupervised classification (Thieler et al. 2009), (Figure 3.)

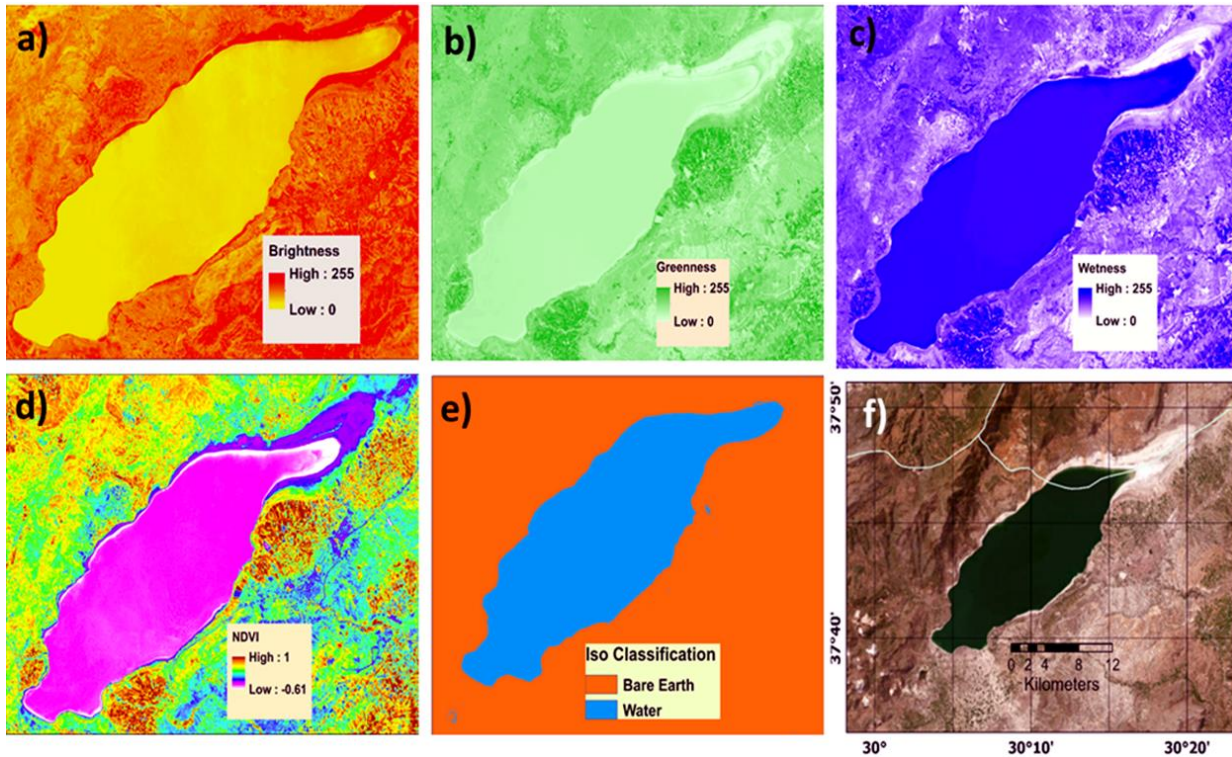


Figure 3. Classification progress of water body extraction (a) Brightness, (b) Greenness, (c) Wetness (d) NDVI (e) ISO Classification (f) satellite image of study area

2.2.2. Extraction of shoreline change rates

In this study, NSM, EPR and LRR statistical methods were used to determine the shoreline changes. Detailed information about periodic and general changes in the coastline can be obtained from these statistical values (Thieler et al., 2009; Nassar et al., 2018). By dividing this distance by time, an EPR statistic can be obtained. The LRR statistic provides data on the time change of all coastlines that intersect a profile line. NSM determines the distance between the oldest and most recent coastline as a statistic, not a rate. The shoreline changes as NSM and EPR statistics requires data from at least two different dates. However, LRR requires all observed time along the shoreline.

The Digital Shoreline Analysis Software (DSAS) 5.0 an extension of the ArcGIS 10.4 software was used to determine shoreline change rates. DSAS software is an image processing and regional change detection method that calculates rate of change statistics from historical shoreline location with multiple multi-temporal Landsat data (Kuleli, 2010; Kuleli, 2011).

A buffer zone that was 500m long and parallel to the shoreline of 2023 in the direction of the lake was determined during the analysis. A total of 1889 transects were built, with each transect having a distance of 25m. In order to accurately calculate the coastline dynamics, the DSAS model requires the uncertainty error value as input. Due to the Landsat data's spectral resolution of 30m, the default data uncertainty value was set to 30m. At the end of the analysis, the statistical values for NSM EPR and LRR values were calculated for lake-to-land and land-to lake positions.

3. Results

In this paper the most recent position of the Burdur Lake evaluated that by using NSM, EPR and LRR statistics of the DSAS tool. The analysis focused on changes for a 10-year period (2013-2023). To evaluate detailed analysis, the period was divided into three intervals: 2013-2017, 2015-2019, and 2019-2023. In this analysis while the EPR and NSM were used for the short-term analysis of the youngest and oldest coastal lines, the LRR indicated a long-term analysis using the least square regression method during the process. Therefore, all shoreline periods from 2013 to 2023 are used for LRR calculation using cyclic trends. Statistical results of these calculations are presented in Table 2. In this table, the rate of shoreline change from land to lake is indicated by the positive values, and the rate of change from lake to land is indicated by the negative values.

According to the finding the maximum land to lake change for the EPR value was obtained as 880.33 m/yr during the period of (2015-2019) and the minimum change movement was revealed as 405.55 m/yr between (2019-2023). On the other hand, the maximum value for EPR was observed at -17.34 m/yr during the 2019-2023 for the lake to land positions. The minimum EPR value for lake to land positions during 2013-2017 was -1.71 m/yr.

According to the LRR value the maximum change rate from lake to land positions was -3.17 m/yr while the change from land to lake was 610.07 m/yr for the years (2013-2023). There was a maximum shoreline movement calculated at 3492.41m for the NSM statistical results in the 2015-2019 period. During the years of 2019-2023, the minimum NSM movement for land to lake positions was 1606.66 m. On the other hand, the maximum NSM movement for lake to land positions was -68.71 m for the years 2019-2023.

Table 2. Statistical results of EPR NSM and LRR along the Burdur Lake shoreline location

| Statistics | 2013-2017 | 2015-2019 | 2019-2023 | 2013-2023 |
|--------------------|-----------|--------------|-----------|-----------|
| EPR | | | | |
| Land to lake | 550.91 | 880.33 | 405.55 | 543.12 |
| Lake to land | -1.71 | -7 | -17.34 | -4.91 |
| Average | 25.39 | 29.98 | 33.68 | 28.47 |
| Standart deviation | 51.07 | 64.76 | 46.63 | 50.42 |
| NSM | | | | |
| Land to lake | 2209.68 | 3492.41 | 1606.66 | 5401.46 |
| Lake to land | -6.85 | -27.77 | -68.71 | -48.82 |
| Average | 101.82 | 118.94 | 133.42 | 283.09 |
| Standart deviation | 204.82 | 256.91 | 184.72 | 501.44 |
| LRR | | | | |
| Land to lake | | | | 610.07 |
| Lake to land | | | | -3.17 |
| Average | | Cyclic trend | | 29.41 |
| Standart deviation | | | | 54.93 |

The study revealed that the movement of land-to-lake change rate in Burdur Lake was more dominant than the movement of lake-to-land. Figure 4 shows the results of EPR, LRR, and NSM values for Lake Burdur during the long-term period (2013-2023) in a general perspective. The maximum net shoreline movement to the land-to-lake in Section 1 was found to be 5401.50 m. In the Section highlighted by number 2, the maximum net shoreline movement in the lake-to-land was -48.90 m. Furthermore, the maximum EPR for lake-to-land was 4.91m/yr and the maximum LRR was -3.17m/yr. in Section 2.

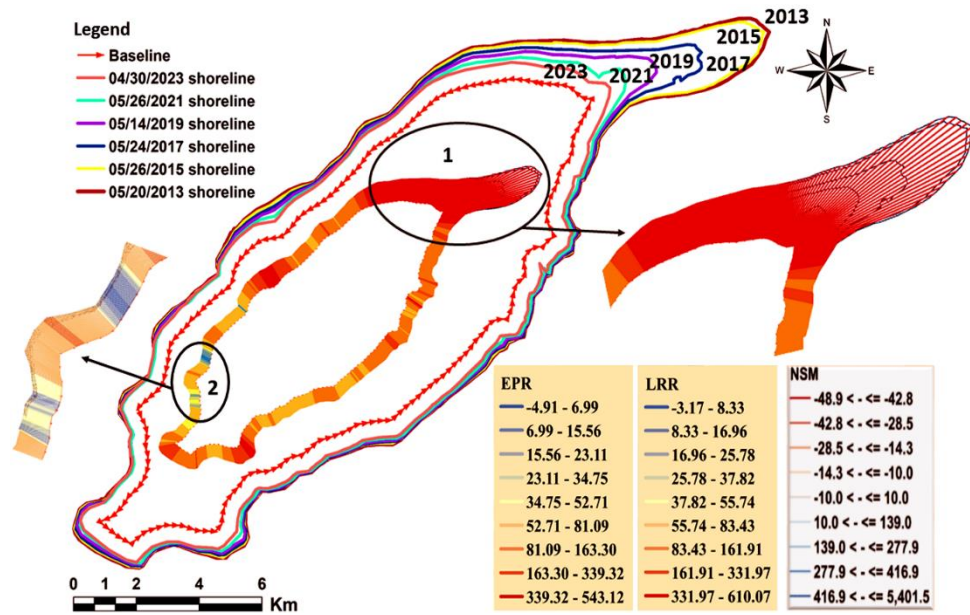


Figure 4. The results of NSM value of Lake Burdur during the period (2013-2023)

The higher shoreline movement of the Lakes, which is mentioned in Figure 4, is shown in Figure 5 with a more in-depth perspective. Figure 5a-b-c shows the EPR, LRR rate of change, and NSM value between 1795 and 1876 transect number. This region has a maximum change from land to lake. In addition, Figure 5d reveals the rate of change value for EPR and LRR in the section of (1795-1876) transects. The graph indicates that EPR and LRR values are very close to each other. The results obtained by EPR and LRR techniques in predicting shoreline change dynamics are very similar (Barik et al., 2019). In this region the maximum shoreline rate of change was 543.12 m/yr for EPR and 610.07 m/yr for LRR in (transect 1810) for land-to-lake (Figure 5 a-c).

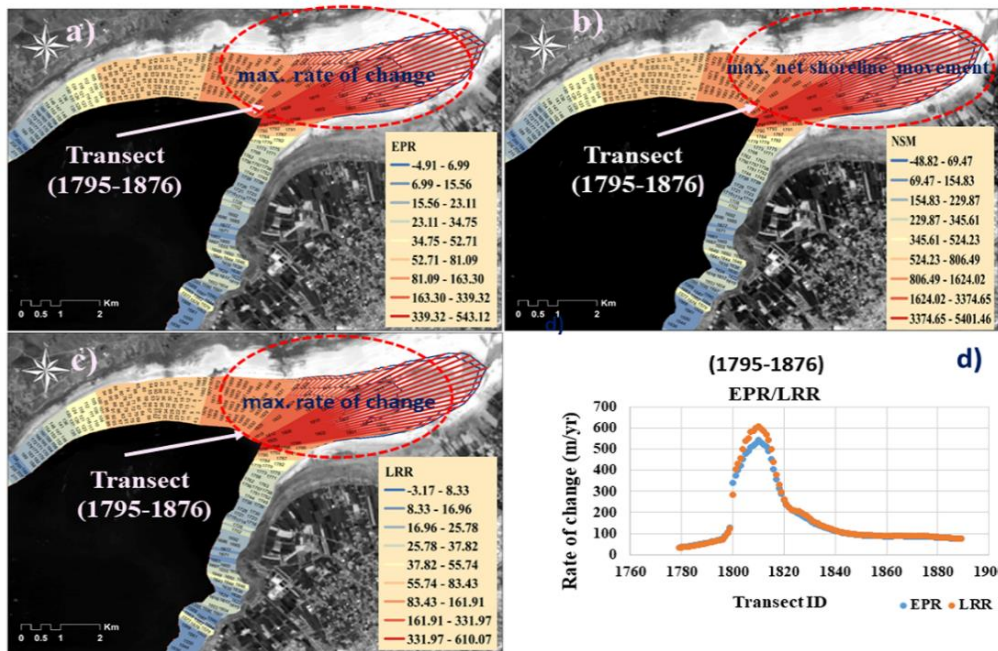


Figure 5. EPR, LRR, and NSM values from the land to lake during the period 2013-2023. (a) EPR values (m/yr) computed for transects (1795-1876) (b) NSM (m) value computed for transects (1795-1876) (c) LRR values (m/yr) computed for transect (1795-1876) (d) The relation of EPR and LRR values (m/yr) computed for transect (1795-1876).

Figure 6 displays a comparison graph between EPR and LRR methods. The regression analysis graph indicated a close relationship between these two methods, resulting in an R-squared value of 0.99m.

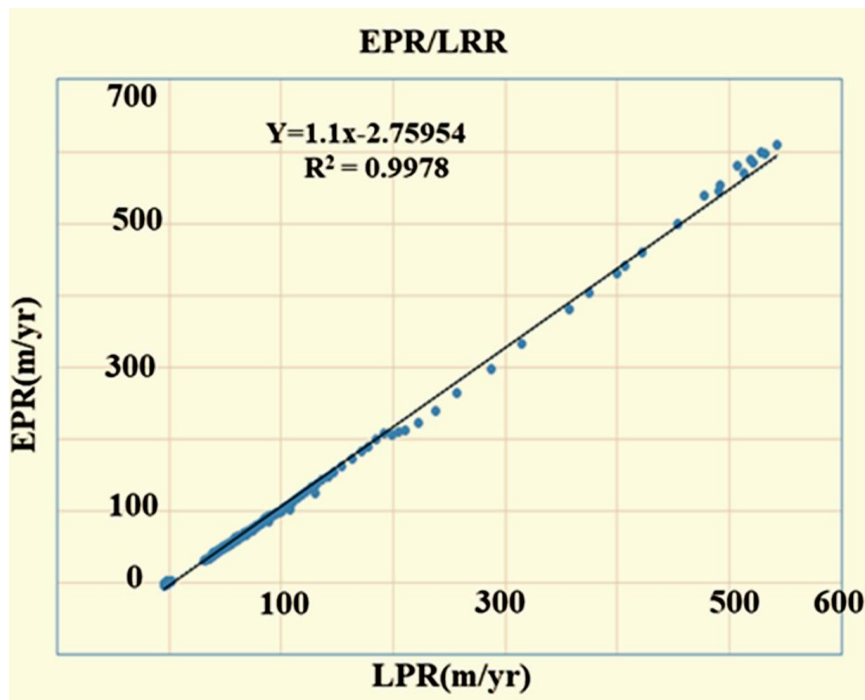


Figure 6. Comparison of EPR and LRR values between 2013 and 2023

The purpose of this study was to determine the future (10- and 20-year) positions of the shorelines in Lake Burdur. In this context, the Kalman Filter approach has been applied to those processes (Kalman, 1960). This approach accepts that a linear regression a good position in the past. The methods use least square by combining the observed shoreline with derived from the model. Consequently, the positional uncertainty of the shoreline was estimated every 10th of a year at each time step. Figure 7 shows the estimated the future positions of Lake Burdur for the time of 2033 and 2043. According to the obtained results it is estimated that the lake would be advance approximately 1560 m in the direction of the lake in 2033 compared to current position and 1400 m in 2043 compared to position of 2033.

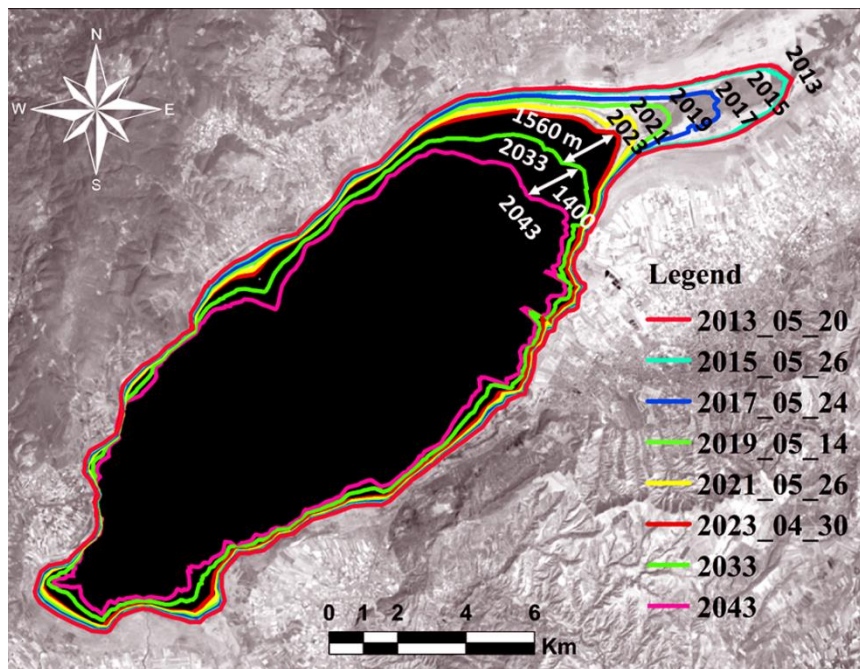


Figure 7. The projected future positions of Lake Burdur for 2033 and 2043 years

Furthermore, results show that the lake area decreased from 139 km² to 118 km² during the period (2013-2023) based on manual digitization from Google Earth images. If the current situation continues, the lake area will

decrease by about 14% by 2033 (101 km²). Moreover, it is predicted that 27% of its current area will be lost within 20 years.

4. Discussion

In this study, possible shoreline rates and positions in Lake Burdur were investigated. The shoreline change of Lake-to-land and opposite direction were evaluated using remote sensing technique and DSAS statistical analysis for the years 2013-2023 and future positions. Especially in the northwest, there is a high number of movements compared to other shoreline environments. Unfortunately, this situation will continue in the future.

As previously mentioned, assumptions in the results section with statistical value may not always be accurate. The findings obtained in this study are calculated entirely based on statistical values. Therefore, many factors could affect the future positions of the lake. The lake level can experience significant changes over time due to both natural and human causes, including global warming, precipitation, streams, groundwater, and tectonic movements. Delta morphology is greatly affected by coastline changes. For example, [Gözükara et al. \(2020\)](#) determined that the temporal and spatial differences between the old and current bottoms are due to differences in the physical and chemical properties of the soil of Lake Burdur. Moreover, slope can be corresponding to the depression floor in the lake topography ([Bahadır & Özdemir, 2011](#)). The negative situation on the shoreline of Burdur Lake may have been influenced by factors such as temperature, precipitation, and drought. According to [Alevyakalı \(2023\)](#), it was observed that the decrease in lake level stopped and even increased in the years following the period of extreme rainfall (2003-2015).

In the literature, there are many studies on Burdur lake current and future shoreline positions. For example, [Sabuncu \(2020\)](#) identified a decline in lake area from 206 km² to 125 km² (40%) over the period. Similarly, [Davraz et al. \(2019\)](#) reported a decrease from 210 km² to 131 km² (37%) over the period (1975-2016). Furthermore, [Şener et al. \(2005\)](#) investigated the period (1975-2002) and calculated a decrease from 210 km² to 153 km² (37%). Moreover, [Hepdeniz \(2020\)](#) has determined that the area of the lake will shrink by about 87.2 km² by 2040 using satellite images. [Sarp & Özçelik \(2017\)](#) found that it lost approximately one-fifth of its area from 1987 to 2011 compared to 1987.

More research is required by researchers to transform this negative situation in the lake into a positive situation in terms of ecology and natural resources. The results of this study showed that the lake region had continued to decline in parallel with the research mentioned in the literature above.

In this study, all calculations were performed with an uncertainty of +-10 m and a confidence interval of 95%. Different results may be produced if the digitization and classification errors have been eliminated on the image or if more accurate image data have been used.

5. Conclusion

Water resources have decreased over the past decade due to global warming, drought, and other environmental effects. The objective of this study is to better understand the position of Lake Burdur and to predict future uncertainties in the 2013-2023 time period. In this context, a remote sensing-based methodology and DSAS analysis are performed to detect these changes. Analysis of the Tasseled Cap and the NDVI spectral indices adopted for the study emphasized the differences between the land and the body of the lake before the DSAS analysis during the process. All those methodologies have been implemented in Lake Burdur, which is also known as Turkey's 7th largest lake with tectonic properties and hosts many bird species. The present research study evaluates shoreline changes for period of from 2013 to 2023 for three different time period (2013-2017), (2015-2019), (2019-2023).

The average rate of shoreline changes, which include EPR, LRR, and NSM rates, was determined using the DSAS extension integrated into ArcGIS software. EPR and LRR statistics were utilized to calculate the maximum shoreline change rates from lake to land and opposite way during the time period and NSM method was used to determine the net shoreline movement. Upon taking into account all the transects, it was observed that the rate of land-to-lake change in Burdur Lake was more dominant than the maximum rate of lake-to-land positions. Consequently, it has been thought that if the negative situations continue, the future positions of Burdur Lake will be worse. This study can be a guide for decision makers by adapting it to better understanding

of coastal dynamics, protection of water resources during the experienced effect of global warming in recent years. Further research can be extended by adding different data sources, such as meteorological and deep topography, based on this study.

Author contribution

The authors of this article contributed to the planning of the study, making the necessary calculations and other processes, interpretation, and preparation of the article.

Declaration of ethical code

We declare that none of the actions specified under the heading "Acts Contrary to Scientific Research and Publication Ethics" have been taken."

Conflicts of interest

The author declares that they have no competing interests.

Acknowledgement

The study is related to a portion of Amine Koç's Master's thesis. The Authors would like to thank the United States Geological Survey (USGS) for the Landsat satellite imagery. We sincerely appreciate all valuable comments from editors and reviewers, which helped us improve the quality of the manuscript.

References

- Adebisi, N., Balogun, A.L., Mahdianpari, M., & Min, T.H. (2021). Assessing the impacts of rising sea level on coastal morpho-dynamics with automated high-frequency shoreline mapping using multi-sensor optical satellites. *Remote Sensing*, 13, 3587. <https://doi.org/10.3390/rs13183587>
- Aishi, A.F., & Hasan, K. (2022). Time-series analysis of landcover dynamics and their relation with coastline migration along Kuakata coast, Bangladesh using remote sensing techniques. *Geology, Ecology and Landscapes*. <https://doi.org/10.1080/24749508.2022.2097374>
- Alevkayalı, Ç., Atayeter, Y., Yayla, O., Bilgin, T., & Akpınar, H. (2023). Burdur Gölü'nde uzun dönemli kıyı çizgisi değişimleri ve iklim ilişkisi: Zamansal-mekânsal eğilimler ve tahminler. *Türk Coğrafya Dergisi*, 82, 37-50. <https://doi.org/10.17211/tcd.1287976>
- Appeaning Addo, K. (2013). Shoreline morphological changes and the human factor. Case study of Accra Ghana. *Journal of Coastal Conservation*, 17(1), 85–91. <https://doi.org/10.1007/s11852-012-0220-5>
- Amrouni, O., Hzami, A., & Heggy, E. (2019). Photogrammetric assessment of shoreline retreat in North Africa: anthropogenic and natural drivers. *ISPRS Journal of Photogrammetry and Remote Sensing*, 157, 73–92. <https://doi.org/10.1016/j.isprsjprs.2019.09.001>
- Ayalke, Z. G., Şişman, A., & Akpınar, K. (2023). Shoreline extraction and analyzing the effect of coastal structures on shoreline changing with remote sensing and geographic information system: Case of Samsun, Turkey. *Regional Studies in Marine Science*, 61, 2352-4855. <https://doi.org/10.1016/j.rsma.2023.102883>
- Ataol, M. (2010). Burdur Gölü'nde seviye değişimleri. *Coğrafi Bilimler Dergisi*, 8(1), 77-92. https://doi.org/10.1501/Cogbil_0000000105
- Ball, G.H., & Hall, D.J. (1965). *Isodata, a novel method of data analysis and pattern classification*. Stanford Research Institute. <https://apps.dtic.mil/sti/pdfs/AD0699616.pdf>
- Bahadır, M., & Özdemir, M.A. (2011). Acıgöl havzasının sayısal topoğrafik analiz yöntemleri ile morfometrik jeomorfolojisi. *The Journal of International Social Research*, 4(18), 323–344. <https://hdl.handle.net/11630/8163>

- Barik, K.K., Annaduari, R., Mohanty, P. C., Mahendra, R.S., Tripathy, J. K., & Mitra, D. (2019). Statistical assessment of long-term shoreline changes along the Odisha Coast. *Indian Journal of Geo Marine Sciences*, 48(12), 1990-1998. <http://nopr.niscpr.res.in/handle/123456789/52790>
- Gülle, İ., Turna, I., Güçlü, S.S., Küçük, F., & Gülle, P. (2008). The vertical profile of water temperature, dissolved oxygen, pH and conductivity in Lake Burdur, Turkey. *Ege University Journal of Fisheries & Aquatic Sciences*, 25(4), 283-287. <https://doi.org/10.12714/egejfas.2008.25.4.5000156609>
- Canbaz, O., Gürsoy, Ö., & Gökçe, A. (2018). Detecting clay minerals in hydrothermal alteration areas with integration of aster image and spectral data in Köseadağ-Zara (Sivas), Turkey. *Journal of the Geological Society of India*, 91, 483-488. <https://doi.org/10.1007/s12594-018-0882-1>
- Canbaz, O., Gürsoy, Ö., & Gökçe, A. (2017). Determination of hydrothermal alteration areas by aster satellite images: Ağmaşat Plato-Zara (Sivas) / Turkey sample. *Cumhuriyet Science Journal*, 38(3), 419-426. <https://doi.org/10.17776/csj.340473>
- Carvalho, R.C., Kennedy, D.M., Niyazi, Y., Cleach, C., Konlechner, T.M., & Ierodiaconou, D. (2020). Structure-from-motion photogrammetry analysis of historical aerial photography: determining beach volumetric change over decadal scales. *Earth Surface Processes Landforms*, 45, 2540-2555. <https://doi.org/10.1002/esp.4911>
- Gözükara, G., Altunbaş, S., & Sarı, M. (2020). Zamansal ve mekansal değişimlerin eski göl tabanlarındaki toprak oluşumu, gelişimi ve morfolojisi üzerine etkisi. *Harran Tarım ve Gıda Bilimleri Dergisi*, 24(1): 96-110. <https://doi.org/10.29050/harranziraat.581874>
- Davraz, A., Şener, E., & Şener, Ş. (2019). Evaluation of climate and human effects on the hydrology and water quality of Burdur Lake, Turkey. *Journal of African Earth Science*, 158, 103569. <https://doi.org/10.1016/j.jafrearsci.2019.103569>
- Dey, M., Sakthivel, P.S., & Jena, B.K. (2021). A shoreline change detection (2012-2021) and forecasting using digital shoreline analysis system (DSAS) Tool: a case study of Dahej Coast, Gulf of Khambhat, Gujarat, India. *The Indonesian Journal of Geography*, 53(2). <https://doi.org/10.22146/ijg.56297>
- Dervisoğlu, A., Yağmur, N., Firatlı, E., Musaoğlu, N., & Tanik, A. (2022). Spatio-temporal assessment of the shrinking Lake Burdur, Turkey. *International Journal of Environment and Geoinformatics (IJEGEO)*, 9(2), 169-176. <https://doi.org/10.30897/ijegno.1078781>
- Hepdeniz, K. (2020). Determination of Burdur Lake's areal change in upcoming years using geographic information systems and the artificial neural network method. *Arabian Journal of Geoscience*, 13, 1143. <https://doi.org/10.1007/s12517-020-06137-5>
- Kalman, R. (1960). A new approach to linear filtering and prediction problems, *Journal of Basic Engineering*, 82(1), 35-45. <https://doi.org/10.1115/1.3662552>
- Kale, M. M., Ataol, M., & Tekkanat, İ. S. (2019). Assessment of shoreline alterations using a digital shoreline analysis system: a case study of changes in the Yeşilirmak Delta in northern Turkey from 1953 to 2017. *Environment Monitoring and Assessment*, 191, 398. <https://doi.org/10.1007/s10661-019-7535-8>
- Kuleli, T., & Bayazit, S. (2022). Development of a method to measure the sustainability of coastal uses. *Environmental Development and Sustainability*, 25(6), 5141-5161. <https://doi.org/10.1007/s10668-022-02259-w>
- Kuleli, T. (2010). Quantitative analysis of shoreline changes at the Mediterranean Coast in Turkey. *Environmental Monitoring and Assessment*, 167(1-4), 387-397. <https://doi.org/10.1007/s10661-009-1057-8>
- Kuleli T. (2011). Automatic detection of shoreline change on coastal ramsar wetlands of Turkey. *Ocean Engineering* 38(10), 1141-1149. <https://doi.org/10.1016/j.oceaneng.2011.05.00>
- Lowe, M. K., Adnan, F.A.F., Hamylton, M., Carvalho, R.C., & Woodroffe, C.D. (2019). Assessing reef-island shoreline change using uav-derived orthomosaics and digital surface models. *Drones*, 3(2), 44. <https://doi.org/10.3390/drones3020044>
- Mishra, M., Acharyya, T., Chand, P., Guimarães Santos, C. A., Kar, D., Das, P.P., Pattnaik, N., Silva, R.M., & Medeiros do Nascimento, T.V. (2021). Analyzing shoreline dynamicity and the associated socioecological risk along the

Southern Odisha Coast of India using remote sensing-based and statistical approaches. *Geocarto International*, 37(14), 3991–4027. <https://doi.org/10.11080/10106049.2021.188200>

- Mitri, G., Nader, M., Dagher, M.A., & Gebrael, K. (2020). Investigating the performance of sentinel-2A and landsat 8 imagery in mapping shoreline changes. *Journal of Coastal Conservation*, 24(40). <https://doi.org/10.1007/s11852-020-00758-4>
- Nassar, K., Mahmod, E.W., Fath, H., Masria, A., Nadaoka, K., & Negm, A. (2018). Shoreline change detection using DSAS technique: Case of north Sinai coast, *Egypt. Marine Georesources Geotechnology*, 37(1), 81-95. <https://doi.org/10.1080/1064119X.2018.1448912>
- Pradhan, B., Rizeei, H.M., & Abdulle, A. (2018). Quantitative assessment for detection and monitoring of coastline dynamics with temporal Radarsat images. *Remote Sensing*, 10(11), 1705. <https://doi.org/10.3390/rs10111705>
- Qiao, G., Mi, H., Wang, W., Tong, X., Li, Z., Li, T., & Hong, Y. (2018). 55-year (1960–2015) spatiotemporal shoreline change analysis using historical disp and landsat time series data in Shanghai. *International Journal of Applied Earth Observation and Geoinformation*, 68, 238–251. <https://doi.org/10.1016/j.jag.2018.02.009>
- Sabuncu, A. (2020). Burdur Gölü kıyı şeridindeki değişiminin uzaktan algılama ile haritalanması, *Afyon Kocatepe Üniversitesi Fen Ve Mühendislik Bilimleri Dergisi*, 20(4), (623-633). <https://doi.org/10.35414/akufemubid.711653>
- Samarawickrama, U., Piyaratne, D., & Ranagalage, M. (2017). Relationship between NDVI with Tasseled cap indices: a remote sensing based analysis. *International Journal of Innovative Research Technology*, 3(12).
- Santra, M., Dwivedi, C.S., & Pandey, A.C. (2023). Quantifying shoreline dynamics in the Indian Sundarban delta with Google Earth Engine (GEE)-based automatic extraction approach. *Tropical Ecology*, <https://doi.org/10.1007/s42965-023-00321-w>
- Sarp, G., & Özçelik, M. (2017). Water body extraction and change detection using time series: a case study of Lake Burdur, Turkey. *Journal of Taibah University for Science*, 11(3), 381-391. <https://doi.org/10.1016/j.jtusci.2016.04.005>
- Survey, U.-U.S.G, Earth Explorer. (2022, 10 January). <https://earthexplorer.usgs.gov/>
- Şener, E., Davraz, A., & Ismailov, T. (2005). The monitoring Burdur Lake water level changes with multi-time monitoring satellite images, (in Turkish). *Türkiye Kuvaterner Sempozyumu (TURQUA-V)* (pp. 148-15). Istanbul.
- Tamer, Y., Berberoğlu, E., & Güllü, İ. (Ed.). (2020). *Burdur'un doğası*. Doğa Koruma ve Milli Parklar 6. Bölge Müdürlüğü.
- Thieler, E., Himmelstoss, E., Zichichi, J., & Ergül, A. (2009). *The Digital Shoreline Analysis System (DSAS) version 4.0. an ArcGIS extension for calculating shoreline change*. US Geological Survey. <https://doi.org/10.3133/ofr20081278>
- TÜİK- Veri Portalı. (2022, 11 Eylül). <https://data.tuik.gov.tr/Kategori/GetKategori?p=Nufus-ve-Demografi-109>
- Wang, H., Xu, D., Zhang, D., Pu, Y., & Luan, Z. (2022). Shoreline dynamics of Chongming Island and driving factor analysis based on landsat images. *Remote Sensing*, 14, 3305. <https://doi.org/10.3390/rs14143305>